PROC. IMPACT 87
Bremen, Germany, 18-22 May 1987

Observation and Modeling of High-Strain-Rate Shear Localization

M. A. Meyers, C.L. Wittman*, H.-r. Pak, and S. Kuriyama**
New Mexico Institute of Mining and Technology,
Socorro, New Mexico, USA

*Permanent address:
Honeywell Defense Systems Division, Hopkins, Minnesota, USA
**Permanent address:
Institute of Physical and Chemical Research, Wako, Saitama, Japan

Introduction

Adiabatic shear localization is a very important phenomenon that has a profound effect on plastic deformation and fracture at high strain rates. The occurrence of shear bands, described qualitatively by Zener and Hollomon [1] for the first time, was quantitatively predicted by Recht [2]. Numerous studies have been devoted to both modeling and observation of shear bands. The computational models developed by SRI-International (SHEAR) are noteworthy in that they incorporate shear instability into the overall deformation process [3]. In spite of the substantial effort devoted to understand shear bands, their detailed nature has not been thoroughly identified yet. This paper describes observations made of the nature of adiabatic shear bands in medium carbon steels and a modeling attempt with the objectives of:

a. Establishing whether there are indeed two classes of shear bands, transformed and deformed, as described in the literature.

b. Identifying the structure of shear bands in steel by transmission electron microscopy and determining their structure in an AISI 4340 steel.

c. Modeling the stress fields at the tip of a shear band in order to establish the conditions for the propagation of shear band by the extension of its tip. The modeling was conducted for HY-TUF steel by using a finite element computational technique.

Observation of Shear Bands

1) AISI 1020 and 8620 steel

These two steels were chosen because they exhibit widely different hardenabilities. The steels were subjected to a variety of treatments to alter, as much as possible, their mechanical response. They were then subjected to ballistic impact by cylindrical projectiles at velocities ranging from 400 to 1000 m/s. The penetration depth as a function of impact velocity is shown in Figure 1. The following treatments were given:

a. 1018 shock annealed: shock hardened (by explosives) and then annealed at 750°C for 15 minutes, producing small grain size.

b. 1018 normalized: austenitizing at 870°C for 30 minutes followed by air cooling.

c. 1018 annealed: annealed for 72 hours and cooled at 10^{o}C/hour.
d. 8620 quenched: austenitizing at 870^{o}C and quenched in brine.
e. 8620 quenche, and tempered at 200^{o}C.
f. 8620 quenched and tempered at 400^{o}C.
g. 8620 aus-tempered: austenitized at 870^{o}C for 45 minutes, quenched into a 500^{o}C salt bath and then air cooled.
h. 8620 annealed.

Shear bands were formed in each of the material conditions. For the conditions with less tendency for shear band formation, higher velocities were required for shear band initiation. The density of shear bands was also sharply dependent on the metallurgical condition. Figure 2 shows optical micrographs of the shear bands for targets and projectile (W-1 quenched and tempered steel). The white etching shear bands are on the left-hand side while the right-hand side shows "deformed" bands. The etchant used was Nital. It can be seen that white etching bands form in the quenched, quenched and tempered, and aus-tempered conditions. These treatments create a structure that is either martensitic or bainitic.

2) <u>AISI 4340 Steel</u>
Adiabatic shear bands, formed in a hollow AISI 4340 steel cylinder subjected to dynamic expansion by means of an explosive charge placed in its longitudinal axis, were characterized. The 4340 steel cylinder was quenched from 695^{o}C and tempered at 230^{o}C for two hours. The resulting hardness was HRC 52. The contained fragmentation test was developed at SRI International and is described by Erlich et al [3]; fragments were furnished by D. Shockey and D. Erlich, SRI International.

Figure 3 shows a scanning electron micrograph of the polished and etched surface of a shear band. The surface features show the structure in a much clearer way than optical micrographs. At the center, there is a horizontal band that etches white. Smaller bands aligned with the martensitic laths can also be seen; they are indicated by arrows. These "incipient" bands would probably not be visible in an optical microscope. They provide important clues on the formation of shear bands. One can also see that the structure within the principal shear band has been altered. The individual martensite laths have been destroyed by plastic deformation. Figure 4 is a montage of high voltage transmission electron micrographs. It shows a region close to a shear band. The plastic deformation of the material is evident from the alignment pattern in the martensite laths. It seems that sliding along the lath interfaces is important.

Figure 5 shows a traverse of the shear band. A boundary in this figure has been drawn to indicate the transition between the matrix and the shear band. As may be seen, this is very arbitrary since no obvious transition between the matrix and the shear band may be observed. This is in contrast to what is

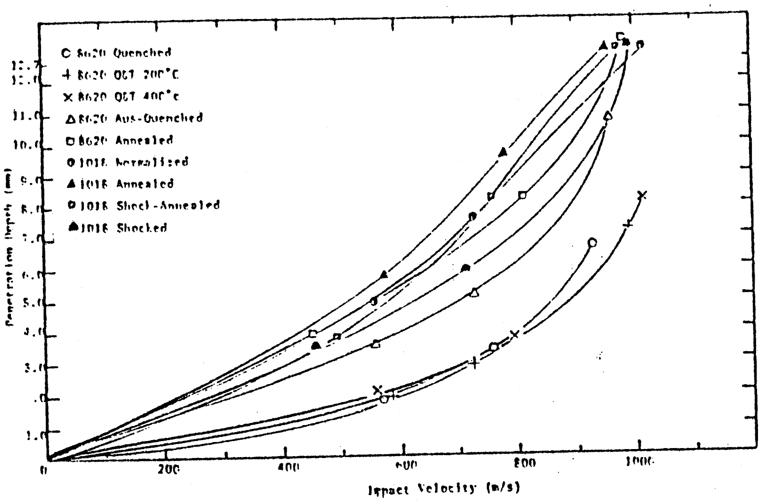

Figure 1. Plot of impact velocity versus measured penetration for ballistic tests.

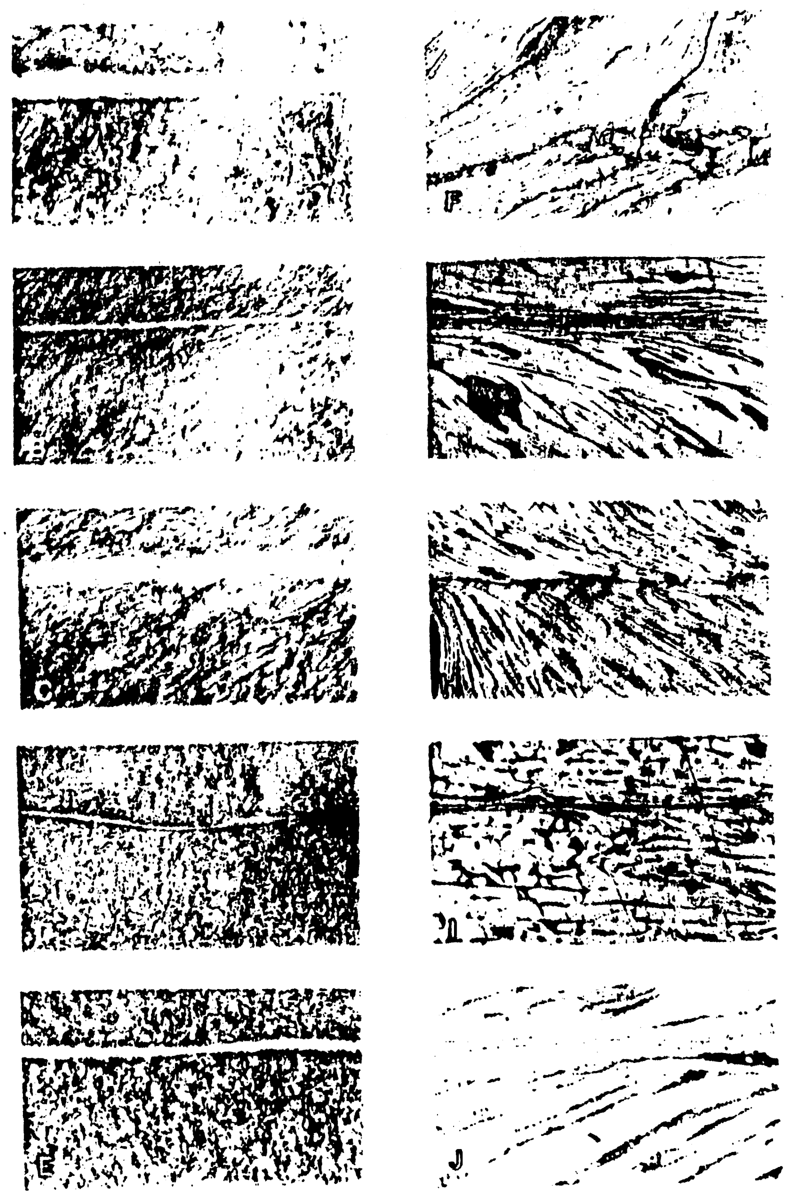

Figure 2. Shear bands formed in the various ballistic tests: (a) AISI 8620 quenched, (b) AISI quenched and tempered 200°C, (c) AISI 8620 quenched and tempered 400°C, (d) AISI 8620 Aus-quenched, (e) W-1 quenched and tempered, (f) AISI 8620 annealed, (g) AISI 1018 normalized, (h) AISI 1018 shocked, (i) AISI 1018 shock-annealed, (j) AISI 1018 annealed.

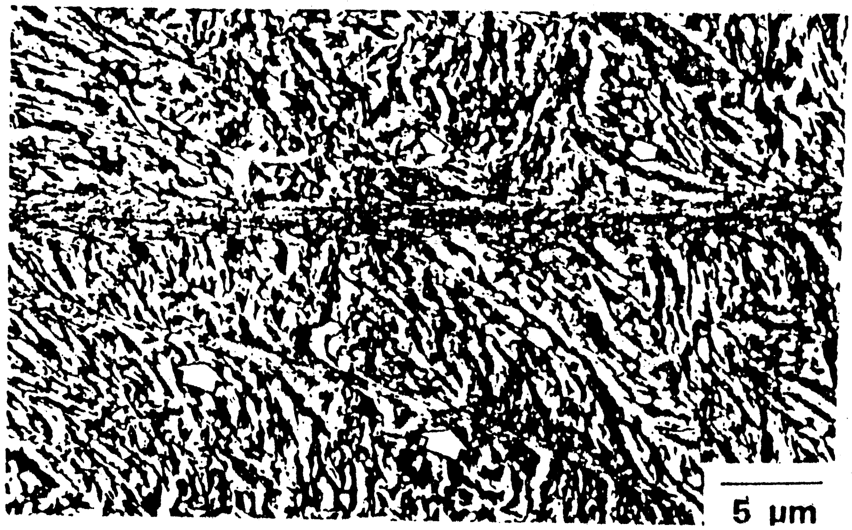

Figure 3. Scanning electron micrograph of a shear band in AISI 4340 quenched and tempered steel. Note that the boundary between the band and matrix is not well defined, and the presence of microbands.

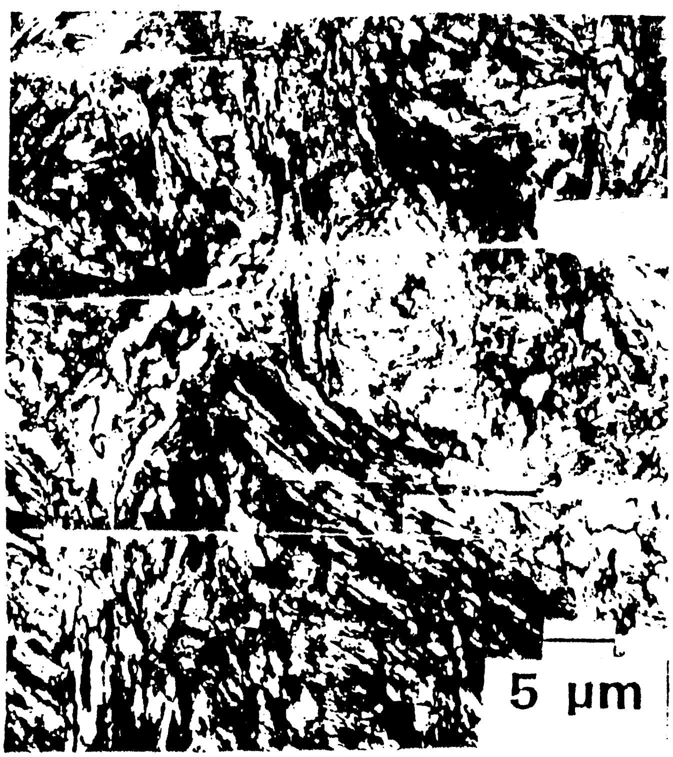

Figure 4. Transmission electron micrograph of incipient band formation in AISI 4340 steel.

observed in titanium and titanium alloys [7,8], where a very definite boundary is observed between the shear band and the matrix. It is, however, consistent with the observations in the optical and scanning electron microscope. The diffraction pattern of the shear band, compared to that of the matrix region, appears to be sharper. This possibly indicates that the shear band has been stress relieved, due to adiabatic heating. The matrix material just beyond the arbitrary boundaries would not have been exposed to the high temperatures, as would have the central portion of the sheared region. They would, however, have been exposed to the same amount of heat, but at a lower temperature for a longer period of time, as the material in the shear band was quenched. The effects of a higher temperature far outweigh the effects of heat present for longer periods of time.

In the center of the shear band, no grain or lath boundaries could be resolved. This is due in part to the interference produced by the large foil thicknesses of up to 5 grains thick. As a result, a large number of moire fringes were observed in the sample, Figure 6. Indexing the electron diffraction pattern from this region revealed that the microstructure contained both martensite and χ carbides.

To aid in the explanation of the microstructures observed, a finite difference model was used to describe the thermal history of the shear band. Heat was deposited in the center of the band until the temperature at some distance from it reached a critical level. This temperature rise was assumed to be $800^{o}C$ and the band width was assumed to be 8 μm. Figure 7 shows the cooling curve of the material on the center of the shear band. The temperature has dropped to close to the original temperature in approximately one milisecond. This is a cooling rate of the order of $10^{5} s^{-1}$. Thus, the cooling rate within the shear band is extremely rapid.

Modeling of Shear Bands

In the analysis presented here, the plastic deformation ahead of a shear band is calculated as a function of imposed displacement. A number of assumptions are required to render the problem tractable. The principal assumptions are:

a. Negligible flow stress in shear band. During the process of propagation, plastic deformation is highly localized in the shear band region, leading to significant temperature increases. Temperatures can approach and possibly exceed the melting point.

b. An adiabatic stress-strain curve represents the plastic deformation process. Since plastic deformation is occurring at a high strain rate, the assumption of adiabaticity is a reasonable one. The use of an adiabatic stress-strain equation was introduced by Olson et al [9] and greatly simplifies computer calculations, allowing one single equation to represent the behavior of the material over a temperature range up to the

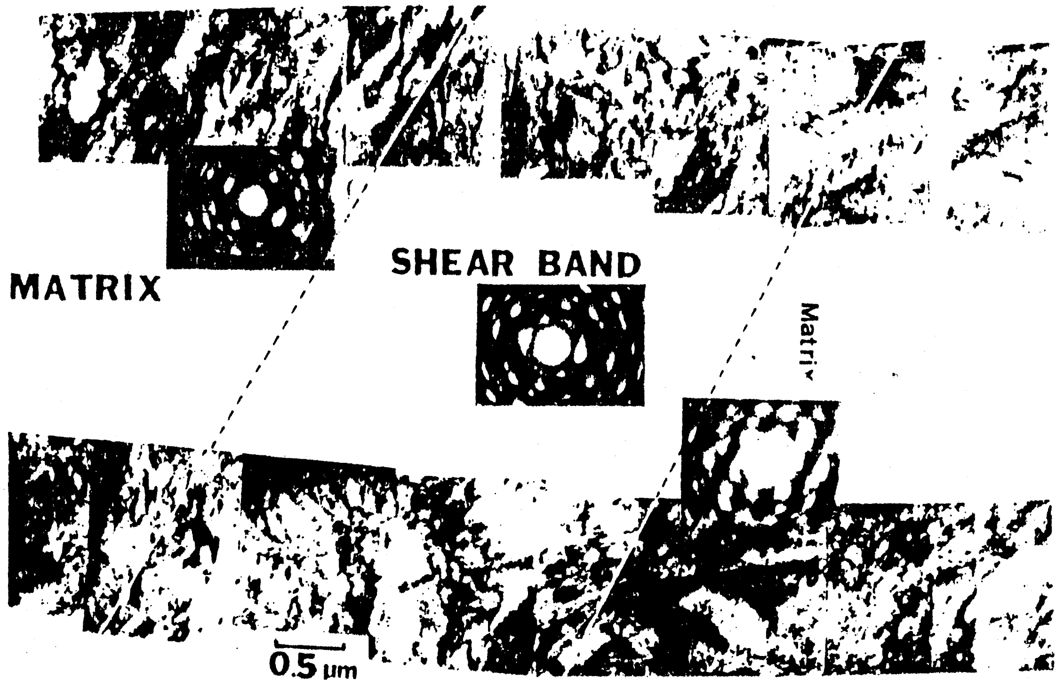

Figure 5. Overall view of a shear band: two traverses of the band are shown.

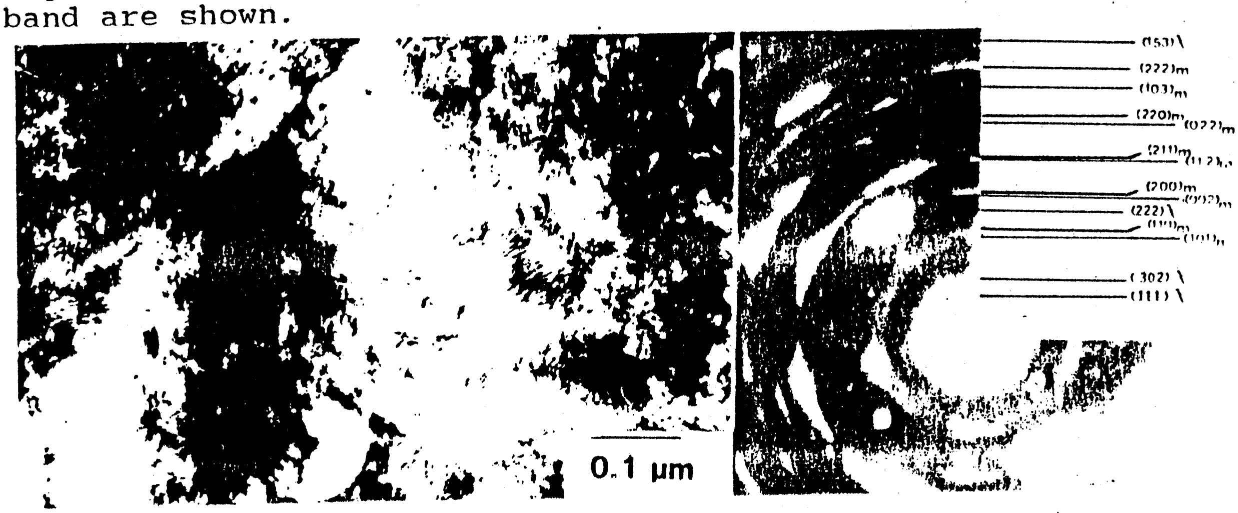

Figure 6. High magnification view (HVTEM) of shear band region.

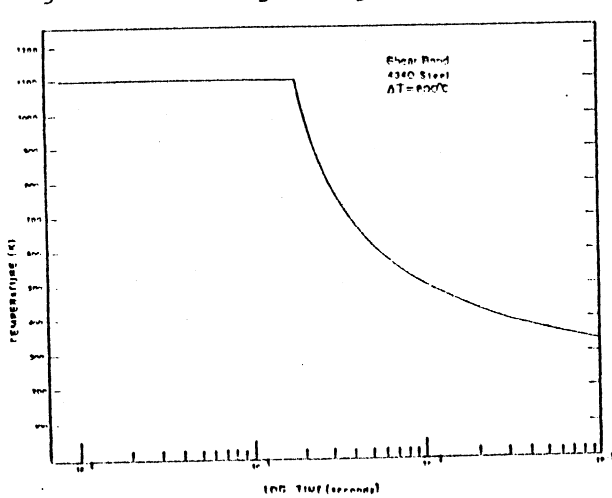

Figure 7. Cooling curve for the center of the shear band in AISI 4340 steel pre-etched by finite differance calculation and a band width of 8 um.

melting point; the strain rate is assumed constant.

c. The body is assumed to be in quasi-static equilibrium throughout the deformation process. As such, wave-propagation effects are absent.

The adiabatic stress-strain curves are characterized by initial work hardening followed by work softening; a plastic instability strain defines the bounds between the two regimes. For the model herein developed, the adiabatic stress-strain curve for a high strength steel determined at a strain rate of $10^2 s^{-1}$ in a torsion test by Olson et al [9] (quenched and tempered HY-TUF steel) was used; it is shown in Figure 8.

In order to compare the propagation of the shear band under an adiabatic condition with the progressive deformation produced under conditions where no instability occurs, a work hardening curve shown by the broken line (Fig. 8) was developed. Up to the instability strain $\bar{\epsilon}_p^i$ it is very close to the adiabatic curve. Beyond instability, the two curves diverge markedly.

These assumptions allow the problem to be modeled by the finite-element method for an elasto-plastic material. The mechanical behavior of the material is assumed to obey the von Mises flow criterion and the incremental theory of Prandtl-Reuss. The code used is an adaptation of Swedlow's [10] code.

Figure 9 shows the isostress and isostrain fields developed after a displacement d is given. The stresses and strains marked along the lines are effective values. It can be seen that although the stress level is fairly high in the whole body (1588-1869 MPa), the plastic strain is concentrated on a narrow band ahead of the notch tip. A thicker solid curve in Figure 9 shows a contour line of $\bar{\sigma}$=1869 MPa and ϵ_p=0.0646; these values correspond to the maximum stress $\bar{\sigma}_{max}$ and the instability strain $\bar{\epsilon}_p^i$ at the transition point on the adiabatic stress-strain curve. The region contained within the isostress line ($\bar{\sigma}$=1869 MPa) is considered to correspond to the shear band. In order to compare the propagation of shear band with the progressive deformation produced in a material which has no instability region, the deformation of the notched body is determined for the stages. Figure 9(b) shows the distribution of effective stress and plastic strain near the notch in the work-hardening material. The deformation of the body and the distributions of stress and strain are almost the same as those in the material of the adiabatic curve except in the vicinity of the notch tip. The isostrain line for $\bar{\epsilon}_p$ =0.0646 is shown by a solid curve in Figure 9(b); this value is equal to the instability strain $\bar{\epsilon}_p^i$ of the adiabatic curve. The stress inside the contour line shown by the solid curve increases with increasing plastic strain. This behavior is the same as that outside the contour, but opposite to that of the adiabatic curve. This contour line reaches a distance of 50 μm from the notch tip when the tangential displacement is 6.87 μm. The concentration of strain within the $\bar{\epsilon}_p^i$ =0.0646 isostrain line, with the attendant reduction of stress, is the critical feature responsible for the propagation of a shear band. By increasing the imposed displacement d, this behavior becomes more and more pronounced; the stress within the instability strain contour line will decrease as d is increased. This drastic difference between adiabatic and isothermal deformation within the $\bar{\epsilon}_p$=0.0646 envelope contrasts with the nearly identical isostress and isostrain contours outside the envelope. This shows that the overall stress distribution is very similar and explains the localization of the shear along a narrow band.

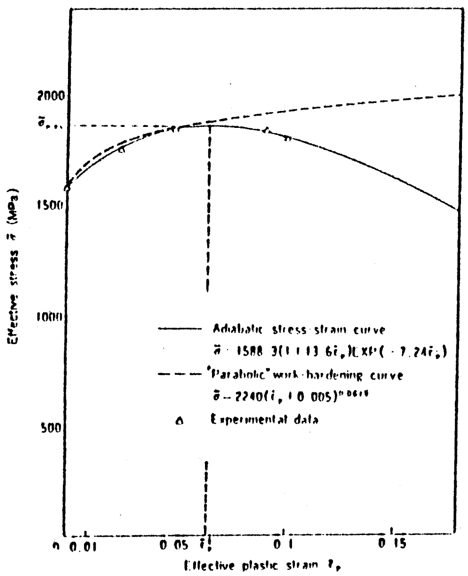

Figure 8. Effective stress-strain curves for HY-TUF steel in quenched and tempered condition.

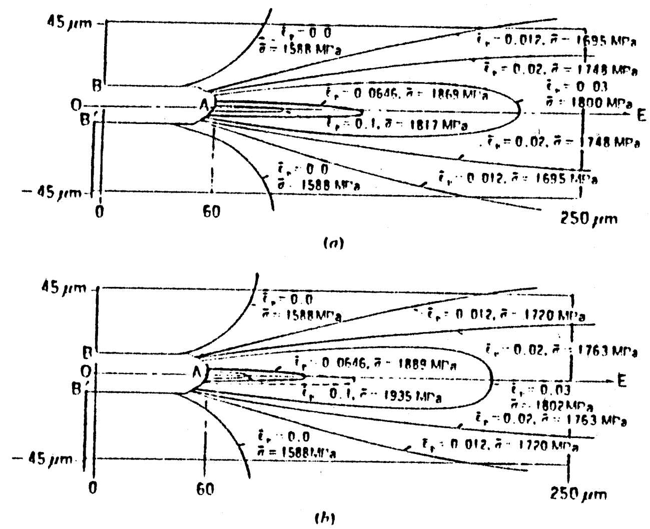

Figure 9. Isostress ($\bar{\sigma}$) and isostrain ($\bar{\epsilon}_p$) contour lines near the notch in material with (a) adiabatic stress-strain curve and (b) isothermal curve.

References

(1). C. Zener, J. H. Hollomon; Journal of Applied Physics, 9(1944)22.
(2). R. F. Recht: Journal of Applied Mechanics, 31(1964)189.
(3). D. C. Erlich, L. Seaman, D. A. Shockey, D. Curran: "Development and Application of Computational Shear Band Model," Final Report, SRI-International, Contract ARBDL-CR-00416, March 1980.
(4). S. Kuriyama, M. A. Meyers: Met. Trans. 17A(1985)443.
(5). C. L. Wittman, M. A. Meyers: Met. Trans., submitted, 1987.
(6). C. L. Wittman: "Microstructural Characterization of Adiabatic Shear Bands in Low and Medium Carbon Steels," M. SC. Dissertation, New Mexico Institute of Mining and Technology, Socorro, NM, 1986.
(7). H. A. Grebe, H.-r. Pak, M. A. Meyers: Met. Trans. 16A(1985)761.
(8). M. A. Meyers, H.-r. Pak: Acta Met. 34(1986).
(9). G. B. Olson, J. F. Mescall, M. Azrin: in "Shock Waves and High-Strain-Rate Phenomena in Metals," eds. M. A. Meyers and L. E. Murr, Plennom, New York, 1981, p. 249.
(10). J. L Swedlow: Computers and Structures, 3(1973)879.